Automatic Resting State Networks Labelling

A DISSERTATION

submitted in partial fulfillment of the
requirements for the award of the degree
of

MASTER OF TECHNOLOGY

in

ELECTRICAL ENGINEERING
(With specialization in Instrumentation & Signal Processing)

By

RAJAT NEGI

(17528009)

DEPARTMENT OF ELECTRICAL ENGINEERING

INDIAN INSTITUTE OF TECHNOLOGY ROORKEE

ROORKEE - 247667

June, 2019

CANDIDATE'S DECLARATION

I hereby declare that this report entitled **Automatic Resting State Networks Labelling**, submitted to the Department of Electrical Engineering, Indian Institute of Technology, Roorkee, India, in partial fulfilment of the requirements for the award of the Degree of Master of Technology in Electrical Engineering with specialization in Instrumentation and Signal Processing is an authentic record of the work carried out by me during the period June 2018 through June 2019, under the supervision of **Dr. R. S. Anand** and **Dr. M. Felix Orlando, Department of Electrical Engineering, Indian Institute of Technology, Roorkee**. The matter presented in this report has not been submitted by me for the award of any other degree of this institute or any other institutes.

Date:
Place: Roorkee (RAJAT NEGI)

CERTIFICATE

This is to certify that the above statement made by the candidate is true to the best of my knowledge and belief.

Dr. R. S. Anand
Professor
Department of Electrical Engineering
Indian Institute of Technology Roorkee

Dr. M. Felix Orlando
Assistant Professor
Department of Electrical Engineering
Indian Institute of Technology Roorkee

Abstract

A 3-D convolutional neural network (3-D CNN) is proposed for the classification of functional brain networks. fMRI technique is widely used to image the neuronal activity (which results in formation of functional networks) while lying static inside a MRI machine. The idea is that the body at rest can simulate the neuronal activity of that when engaged in extrinsic tasks. The study of neural activity is significant for understanding the working of brain. It is believed that low-frequency fluctuations observed in the BOLD signals reflect the spontaneous neural activity and that the synchronized fluctuations in distinct brain regions, therefore, point to functional connections between them. Different functional connectivity networks have been found, and these networks change in patients with multiple pathologies (neurological, psychiatric). Determination of networks correctly is essential for getting in depth understanding of brain functioning or understanding the differences between brain region connectivity of a normal being and a patient for diagnostic and clinical purposes. Machine learning techniques became very popular in the field of resting state fMRI network based classification. However, the application of convolutional neural networks has been proposed only very recently and has remained largely unexplored.

A 3-D CNN is designed to classify the functional networks with more speed and accuracy.

Acknowledgements

I would like to express my deep sense of gratitude and sincere thanks to my supervisors **Dr. R. S. Anand** and **Dr. M. Felix Orlando**, Department of Electrical Engineering, Indian Institute of Technology Roorkee, for their valuable guidance and support. I am highly indebted to them for their encouragement and constructive criticism throughout the course of this project work.

I would also like to thank **Mr. Yogesh Sariya** who provided me his constant guidance and helped me in better understanding of the field subjected to my study.

I would like to thank **Rethink! (The Tinkering Lab of IIT Roorkee)** for providing me with the needed support of the hardware (workstation) in their facility.

Contents

List of Figures

List of Tables

Abbreviations

ABIDE	**A**utism **B**rain **I**maging **D**ata **E**xchange
AD	**A**lzheimer's **D**isease
ASD	**A**utism **S**pectrum **D**isorder
BOLD	**B**lood **O**xygenation **L**evel **D**ependent
CCS	**C**onnectome **C**omputation **S**ystem
CNN	**C**onvolutional **N**eural **N**etwork
CSF	**C**erebrospinal **F**luid
DMN	**D**efault **M**ode **N**etwork
EPI	**E**cho**P**lanar **I**maging
FCP	**F**unctional **C**onnectome **P**roject
fMRI	**f**unctional **M**agnetic **R**esonance **I**maging
GICA	**G**roup **I**ndependent **C**omponent **A**nalysis
HCP	**H**uman **C**onnectome **P**roject
HRF	**H**emodynamic **R**esponse **F**unction
ICs	**I**ndependent **C**omponents
ICA	**I**ndependent **C**omponent **A**nalysis
MCI	Mild **C**ognitive **I**mpairment
MRI	**M**agnetic **R**esonance **I**maging
N-ICs	**N**oise **I**ndependent **C**omponents
NITRC	**N**euro**I**maging **T**ools and **R**esources **C**ollaboratory
PCP	**P**reprocessed **C**onnectomes **P**roject
PET	**P**ositron **E**mission **T**omography

RsfMRI	**R**esting **s**tate **f**unctional **M**agnetic **R**esonance **I**maging
RSN	**R**esting **S**tate **N**etwork
S-ICs	**S**ignals of Interest **I**ndependent **C**omponents
SICA	**S**patial **I**ndependent **C**omponent **A**nalysis
TC	**T**ypical **C**ontrols

Chapter 1

Introduction

The human brain is composed of anatomically connected systems which works in parallel with task specific interacting regions of brain and continuously communicating with 11 organ systems of the body for proper functioning of the biological being that we are. The human brain is the most complex machine in the physical universe. Studying the connectivity of the systems of the brain research efforts have been focused on improving the understanding of the functioning of this sophisticated machine to gain insights on cognition, thinking, involuntary tasks, behaviour and subconscious. Functional connectivity represents a novel approach which enables to explore the neuronal activity of brain regions that are functionally connected when they may or may not be anatomically distant. The extraction of functional networks from fMRI data has became very much popular from more than two decades. Functional connectivity MRI (fcMRI) measures the intrinsic functional correlations between brain regions (KR et al., 2010; S et al., 2013). The method functional imaging using MRI is sensitive to the entanglement of both distributed as well as adjacent areas (Biswal et al., 1995). Physiological fluctuations in resting brain observed using echo-planar MRI (EPI,MRI) consists of low-frequency signals (< 0.1 Hz) resulting due to correlation of neuronal activity with both rCBF (regional cerebral blood flow) and blood oxygenation (Biswal

et al., 1995). Typically, tens or hundreds of concurrent functional networks can be effectively and robustly extracted from whole-brain functional magnetic resonance imaging (fMRI) data of an individual using independent component analysis (ICA).

1.1 Literature Survey

Magnetic Resonance Imaging (MRI) is the most widespread and popular imaging technique used for clinical and research applications due to its non invasiveness and absence of any ionizing radiation. Its success is mostly due to at least three factors: 1) sensitivity of MR signal to various physiological parameters distinctive to living tissues (such as diffusion properties of H20 molecules, relaxation time of proton magnetization or blood oxygenation) resulting in a vast panoply of MRI modalities; 2) constant hardware improvements (e.g. mastering high field homogeneous magnets and high linear magnetic field gradients allows an increasing of spatial resolution or a reduction of acquisition time respectively); and 3) sustained efforts by researchers to develop robust software: for image processing (to de-noise, segment, fusion, realign or visualize brain images), for computational anatomy leading to exploration of brain structure modifications during learning, brain development or pathology evolution and for time course analysis of functional MRI data. Statisticians play a key role in this last factor since data produced are complex: noisy, highly variable between subjects, massive and, for functional data, highly correlated both spatially and temporally (Bordier et al., 2010). The fact that changes in regional cerebral blood flow (rCBF) resulting in fluctuations in blood oxygenation (Biswal et al., 1995) is utilised to image the brain activity continuously during a task, behaviour or emotion. This procedure is known as functional Magnetic Resonance Imaging (fMRI). The fMRI signal is detected due to changes in magnetic suseptibility of blood during neuronal firing. It is a indirect non-invasive detection of brain activity : the detected signal is filtered by hemodynamic response function (HRF) and the neuro-vascular coupling is only partially explained (Bordier et al., 2010; NK and

J., 2004). Originally observed using positron emission tomography (PET) in between-subject variation, functional correlations among widely distributed brain regions are consistently observed in analyses of fMRI time series data (MD et al., 2007). As (Friston, 1994) noted in his exposition of functional connectivity, the repeated scans acquired in quick succession with fMRI provide an abundant source of information about correlated activity in brain regions. The earliest experiments regarding fMRI showed that time course of BOLD signal from a region in the motor cortex was strongly correlated with the contralateral motor region and the midline regions of motor system (Biswal et al., 1995). The coherent fluctuations were immediately observed within individual participants, indicating that the method is highly sensitive and raising the possibility of computing individual differences (KR et al., 2010). Unlike earlier approaches focusing on stimulus-evoked modulations gaining insight to functional connectivity, the correlated activity observed by (Biswal et al., 1995) were manifest while participants rested passively without any detectable movement, suggesting the fluctuations were chiefly driven by intrinsic activity events constrained by anatomy (KR et al., 2010). Since the seminal observation of Biswal and colleagues, multiple systems of brain have been demonstrated to exhibit functional correlation at rest including the visual and auditory systems, the default network and the medial temporal lobe memory system, the language system, the dorsal attention system, and the frontoparietal control system (KR et al., 2010). These observation strongly evince the presence of functional networks in the brain at rest or task-negative/positive states and varied states of consciousness. These intrinsic activities of brain are often measured at rest so the functional networks are identified as resting state networks (RSNs). The fMRI procedure during rest or passive fixation has the advantage of minimising the external fluctuations and can be performed easily. The clinical applications of fMRI derived functional networks got highlighted shortly after the their extraction and understanding the connection between intrinsic networks and brain regions integrity in normal patients (Biswal et al., 1998). The basic idea is to utilise correlation strengths between functionally linked regions as a marker for brain systems connectivity and integrity. This approach has come out to be a powerful technique for mapping differences in neurological and psychiatric

disorders. (Greicius et al., 2004) demonstrated that functional connectivity within the default network is disrupted in patients with Alzheimer's disease (AD) in comparison with normal older controls. Connectivity disruptions were further detected in mild cognitive impairment (MCI) and in cognitively normal older individuals who harbor the pathology of AD. These observations indicate that the method is sensitive and of potential diagnostic value. Functional disordering has been reported for a number of neuropsychiatric disorders including autism, attention deficit hyperactivity disorder, depression, and schizophrenia (KR et al., 2010). There are several methods that had been developed to extract information from the raw fMRI data : voxel based, region of interest (ROI) based, graph theory, independent component analysis, and machine learning methods (Vergun et al., 2016). Out of these methods, ICA is the most popular method for the extraction of functional network spatial maps from the raw fMRI data. It is a statistical technique that does not involve any priori information only with the assumption that the components are statistically independent and allows multivariate fMRI signal to decompose into additive voxel activated components. These activated components represents various spatial maps which may correspond to functional networks or some physiological activity or noises present in the data. To aid the mapping of the brain region functioning for researches and clinical applications the spatial maps from the application of ICA should be labelled and organized. The process of labelling the functional networks is a very manual task and prone to inter-expert preferences which is very time consuming and having high probability of inaccuracy. To fulfil the necessity of automated labelling process methods of template matching through correlation strengths and machine learning methods are commonly used. However, this task of automation of functional networks labelling process is still challenging due to enormous variability of presence of various types of functional networks and noises (Zhao et al., 2018). Advanced machine learning techniques like deep learning Convolutional Neural Networks (CNN) provides superior capability in recognising and representing spatial patterns dealing with huge variability and noises. The CNN technique popular with 2-D images with multiple channels for different purposes of classification, regression or segmentation when extended in 3-D framework shows a great effectiveness and

robustness in accurate classification of functional brain networks (Zhao et al., 2018).

1.2 Obejectives of Dissertation Work

The objectives of this dissertation work includes :

1. Extracting the functional networks from the preprocessed fMRI data
2. Segregation of Functional Network Spatial Maps from Physiological Acivity and Imaging Artifacts
3. Proposing and Implementation of 3D-CNN architecture
4. Evaluation and performance of the proposed structure from the conventional techniques for automatic labelling

Chapter 2

Extraction of Functional Networks from fMRI Data

2.1 Experimental Dataset

The RsfMRI data used for the preparation of proposed model is taken from the Preprocessed Connectomes Project (PCP). The open share of preprocessed neuroimaging data from Autism Brain Imaging Data Exchange (ABIDE) is used with entire phenotypic and scanning details. It is a initiative under the 1000 Functional Connectomes Project (FCP) and International Neuroimaging Data- sharing Initiative (INDI). The data present in the ABIDE is a collection of 16 international imaging sites that have aggregated and openly share neuroimaging data from 539 individuals suffering from Autism spectrum disorder (ASD) and 573 typical controls (TC). These 1112 datasets are composed of structural and resting state functional MRI data along with phenotypic information. The data used for this experimental work is utilised from that shared by **University of Leuven** and **Social Brain Lab - Netherlands Institute for Neuroscience**. The participants belong to different age, diagnostic and gender groups. The summary of the demographics is given below:

Table 2.1: Demographics of Participants

	ASD	TC
Adolescent		
Mean Age	13.92	14.34
Age Range	$12.1 - 16.8$	$12.2 - 16.9$
Gender	$12M/3F$	$15M/5F$
Adults		
Mean Age	35	33.733
Age Range	$22 - 64$	$20 - 42$
Gender	$15M/0F$	$15M/0F$

2.2 Image Preprocessing

The preprocessing step of the fMRI data is the stage at which some operations are done on the fMRI images to detect and repair potential artifacts that may be caused either by the MRI scanner or by the person being scanned itself. Various types of artifacts to be corrected at the preprocessing stages include (Poldrack et al., 2011):

- Spikes - Brief changes in brightness due to electrical instability in scanner.
- Ghosting - When there is a slight offset in phase between different lines of K-space in an echo planar acquisition or due to periodic motion such as heartbeat or respiration.
- Distortion - Due to inhomogeneity of main magnetic field caused by the air-tissue interfaces.
- Slice-time differences - The data acquired to form the MRI images, various 2D slices are taken at systematically different times, with differences ranging up to several seconds.

- Motion deformity - Mismatch of the location of subsequent images taken in time with head motion. Another head motion related artifact can result into disruption of the MRI signal itself due to the protons that move into a voxel from a neighboring slice have an excitation that is different from that expected by the scanner, and the reconstructed signal will not accurately reflect the tissue in the voxel; this is known as a spin history effect (Friston et al., 1996).

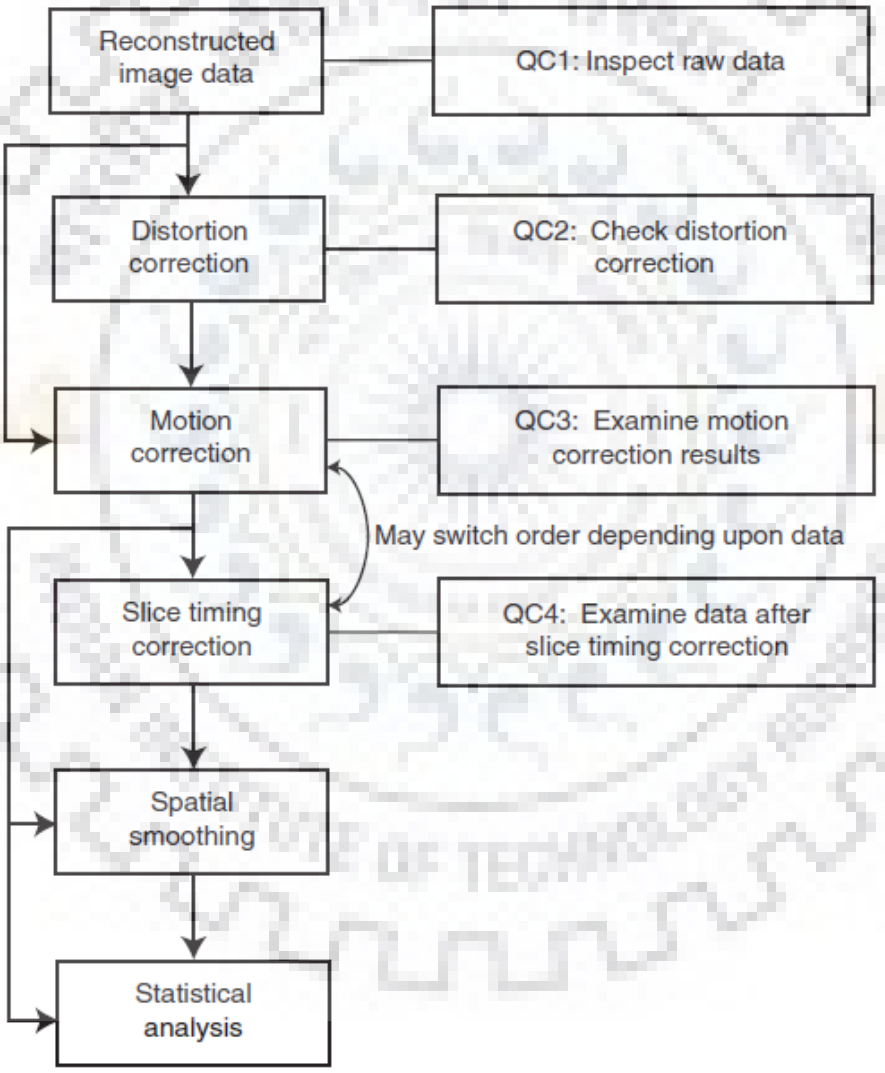

FIGURE 2.1: An overview of the standard fMRI preprocessing stream. With the exception of motion correction, the rest of the preprocessing steps can be viewed as optional, and their use will depend upon the needs of the study and the available data (Poldrack et al., 2011)

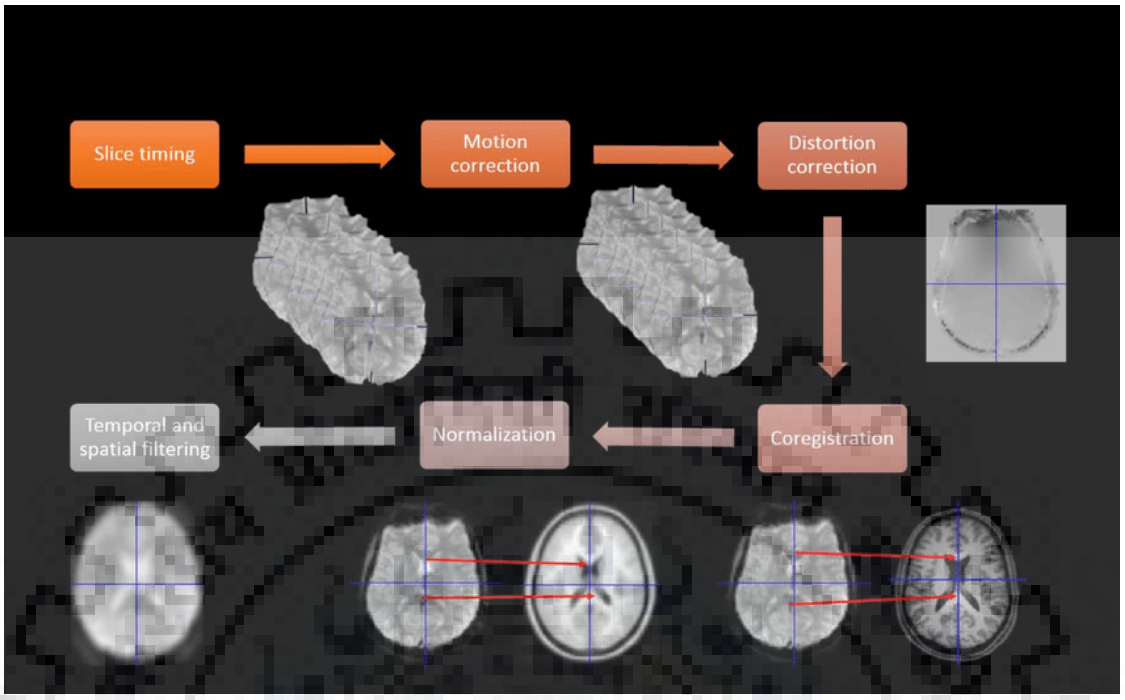

FIGURE 2.2: A pictorial representation of preprocessing steps (Fengler, 2016)

Preprocessing of fMRI images varies substantially with different software packages and laboratories. In this work the fMRI data taken is already preprocessed at Preprocessed Connectomes Project (PCP) (Craddock and Bellec, 2019) using data of ABIDE at `https://www.nitrc.org/projects/fcon_1000/` as per the connectome computation system (CCS) protocol which starts with skipping of initial 4 volumes and then denoising, motion realignment, slice-timing correction and 4D intensity normalization is done. After these initial processes the functional images are registered to **MNI152** standard templates (combining boundary based co-registration). The whole procedure can be found at `http://lfcd.psych.ac.cn/ccs.html` .

2.3 Decomposition of fMRI data

After the preprocessing of the raw data a statistical model is developed to find the regions where the model explains the data illustratively. These statistical models are

developed to detect the systematic patterns in the preprocessed data. These methods try to decompose the 4D data into some set of spatio-temporal components that are additive in nature in different proportions to obtain the original signal. One such method is Independent Component Analysis (ICA) which is a statistical technique used to decompose a multivariate signal into its additive subcomponents with the assumption that the components are statistically independent. The decomposed components are again very useful in detecting artifacts or noise signals and the functional networks can be separated from them. The preprocessed fMRI data is decomposed through spatial ICA (SICA) technique in Group ICA fMRI Toolbox (Egolf et al., 2004). The Independent Component Analysis step is done on the whole group of the participants in the study to find smoothed, agregate and normalised spatial maps of the functional networks. The order of the model of 100 was selected for decomposition. The FASTICA algorithm was used to breakdown the fMRI data (Tichavsky et al., 2006). The components which resulted from ICA application represent group components and so the back reconstruction step is added for the final representation of the resultant components to compute individual subject components (or functional networks in addition to noise components).

Chapter 3

Identification of Functional Network Spatial Maps

3.1 Signals in ICA Decomposed Components

After the decomposition of fMRI data using Independent Component Analysis a number of characteristic components gets separated which are composed of signals of interest and various artifacts. Artifacts primarily related to motion and physiology deteriorates the functional signal-to-noise ratio. ICA then helps to separate the neural signals, structured noise and random noise from the fMRI images. The signals of interest or neural signals must be separated out from the noise present in the data to further the analysis of the functional networks activated in the brain. Accurate identification of the neural signals should be carried out to reduce the error or getting wrong conclusions at the stage of utilizing functional networks.

3.2 Large Scale Brain Networks

The large scale brain networks are a collection of constellation of brain regions which when activated forms the functional networks. The functional networks are basically formed from the activation or deactivation of synchronised brain regions signaling various functions performed by the biological machinery. Various functional networks were identified and named during the time course from the beginning of the RSN study. Some of the typical large scale brain networks include:

TABLE 3.1: Various Functional Networks of the Brain

Resting State Functional Networks	**Interacting Regions**
Default Mode Network	Posterior cingulate Cortex; Medial Prefrontal Cortex; Angular Gyrus; Temporopareital junction; Lateral Temporal Cortex; hippocampus; parahippocampus; posterior inferior parietal lobe
Sensorisensory Network	Post Central Gyrus; Pre central gyrus; Supplementary motor area
Auditory Network	Superior temporal gyrus; Heschl's gyrus; Insula; Postcentral gyrus
Visual Network	Occipito temporal regions; striate cortex; polar visual areas
Basal Ganglia Network	base of the forebrain and top of the midbrain; globus pallidus, ventral pallidum, substantia nigra, and subthalamic nucleus, straitum
Fronto-pareital Network	Inferior frontal gyrus; medial frontal gyrus; precunneus; inferior parietal; angular gyrus

The various spatial maps of the resting state networks reported and developed by the researchers in their study helps to easily learn the brain regions associated with the extracted components. Some of the large scale brain networks were thoroughly assessed by (Smith et al., 2009) in correspondence to BrainMap `http://www.brainmap.org/` database of resting state networks.

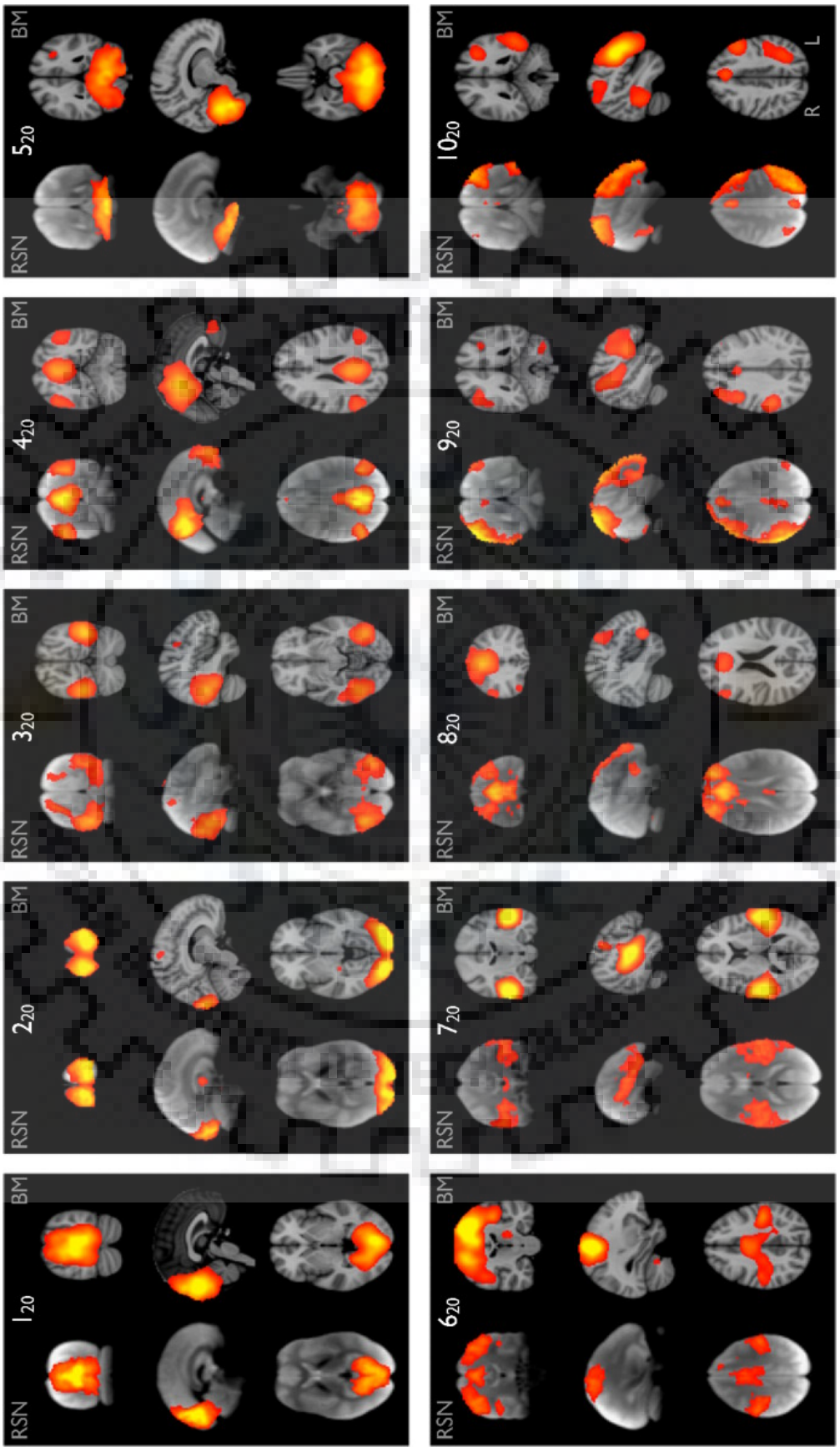

FIGURE 3.1: Ten large scale brain functional networks as reported in (Smith et al., 2009) study.

In fig 3.1 shows the well matched 10 pairs of the resting state networks obtained from ICA decomposition of 36 subjects fMRI scans with a dimensionality of 20. Left column of each pair figure corresponds to the resting state fMRI data of subjects group mean superimposed on mean fMRI images of all subjects. Right column of each pair figure corresponds to the networks from BrainMap superimposed on the MNI152 standard template images. Maps 1, 2 and 3 ("visual") shows medial, occipital pole, and lateral visual areas. Map 4 ("default mode network") occupies medial parietal, bilateral inferior–lateral–parietal and ventromedial frontal cortices. Map 5 ("cerebellum") includes the cerebellum. Map 6 ("sensorimotor") occupies supplementary motor area, sensorimotor cortex, and secondary somatosensory cortex. Map 7 ("auditory") is incorporated with the superior temporal gyrus, Heschl's gyrus, and posterior insula. Map 8 ("executive control") includes several medial–frontal areas. Maps 9 and 10 ("frontoparietal") occupies several frontoparietal areas (Smith et al., 2009).

3.3 Manual Labelling of Decomposed Components

The independent components (ICs) after the ICA contains noise signals (N-ICs) and signals of interest/ neural signals (S-ICs). There are a number of approaches for labeling ICs investigated by the researchers. These approaches can be classified according to

1. whether ICA is performed on individual fMRI scan or is performed through a single, "group ICA" on group fMRI scans

2. whether the approaches are entirely automated or are "manual", requiring element of visual inspection and human decisions

3. whether the approaches are entirely data driven or require some task-related temporal or spatial (brain regions) information

4. and whether the approaches are based on Independent Components's temporal or spatial features, or both.

IC time courses and their associated Fourier frequency spectrums are used to distinguish N-ICs from S-ICs. The characteristics of these parameters to identify it as a noise component include abrupt, large shifts in time course (spikes); oscillating, "quasi-periodic" pattern; similarity to white noise; similarity to time courses of activations from regions of the brain where neural activity does not occur (ventricles and vasculature); similarity to task-related activity; heteroscedacticity in residuals from regressing IC time courses against a task-related time course; and relative amount of power at frequencies considered typical for artifacts (Kelly et al., 2010). Details to be taken care of at the time of visual inspection of independent components (ICs) to denoise the fMRI data and label them correctly include (Kelly et al., 2010).:

- Degree of association of activation in CSF, white matter, gray matter and/or blood vessels.
- Extent of components presence in brain periphery.
- Degree of clustering and scattering of thresholded voxels in IC spatial networks.
- Degree of similarity with constellations of brain regions known to perform particular functions.

Components are labelled Noise when:
IC shows "activation" or "deactivation" predominantly (90% or more) in peripheral areas or in a spotty or speckled pattern, seemingly scattered randomly over a large volume (roughly 1/4th or more) of brain without consideration for functional-anatomical boundaries.

Components are labelled Signals when:
At least 10% of the activation or deactivations are found in small (roughly 25 voxels of 4x4x4 mm) to larger gray matter clusters localised to small regions of brain rather being diffusely scattered across large volumes found in periphery.

In cases regarding doubt whether more than 90% of a component represents noise, the general rule is to label it S-IC; but if it also seems likely that the component represents at least 90% noise, then the component is labeled as N-IC if and only if one or more of the following conditions apply (Kelly et al., 2010).:

- High frequencies: More than 50% of power in the Fourier frequency spectrum of the component lies above 0.1 Hz. This cutoff frequency is appropriate for resting-state functional connectivity studies (D Greicius et al., 2007) and may be modified accordingly for studies focusing on different frequency range of neural signals.
- Spikes: One or more large (greater than five standard deviations), abrupt (over six seconds or less) changes in the normalized time course.
- Sawtooth pattern: Sharp and alternate spikes in the time course of the IC resembling a sawtooth pattern.
- Sinus co-activation: Roughly ten or more threshold voxels present in the superior sagittal sinus.

Manual study of the resting state networks obtained from the IC after the process of GICA resulted in identification of S-ICs and N-ICs. After the identification of S-ICs proper recognition of the functional network is done carefully via human visual and intellectual input. Some of the manual labels of the IC are reported next.

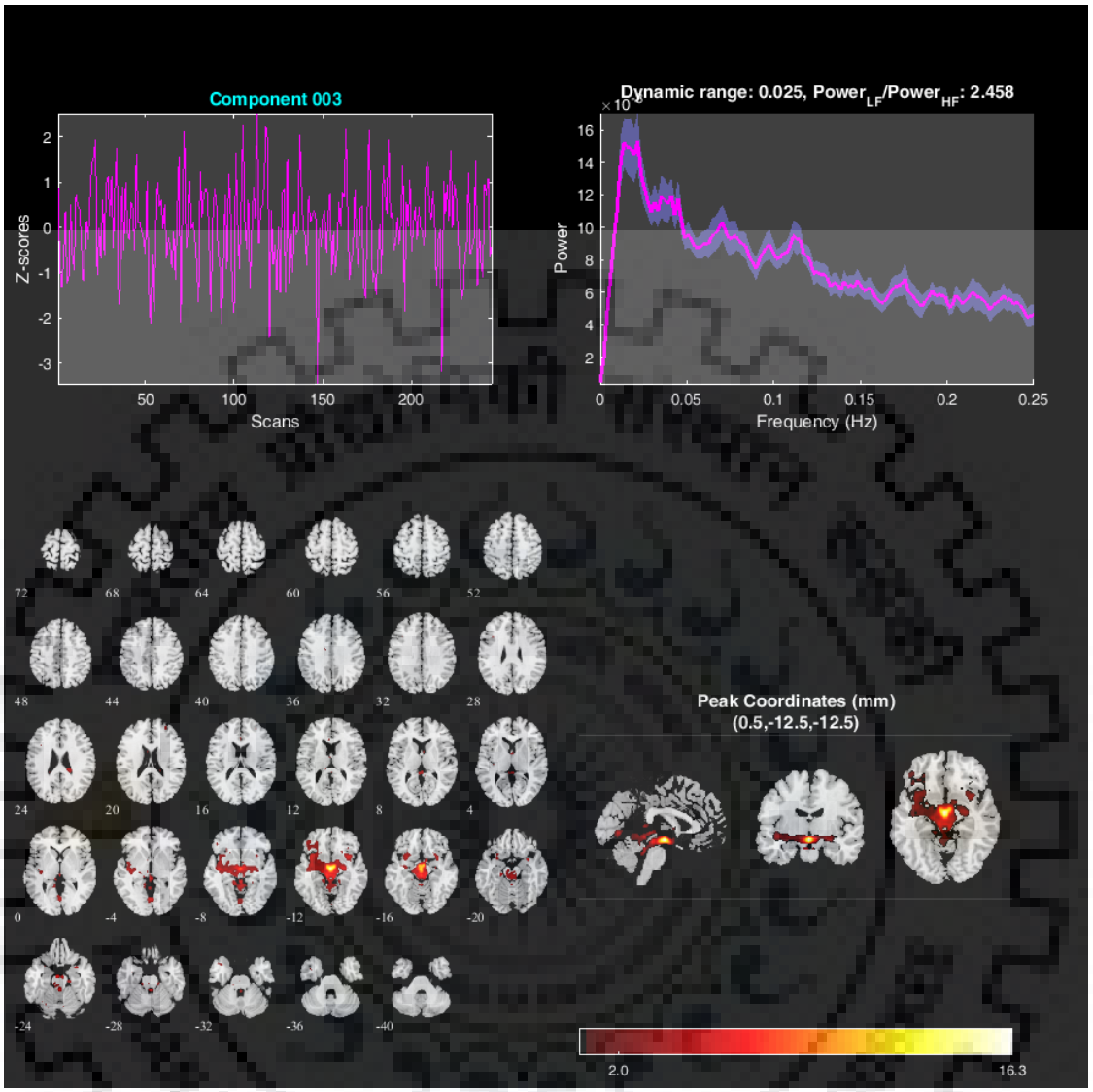

FIGURE 3.2: The label identified for this IC through template matching is visual network. But this IC is noise as the component is scattered to CSF and white matter and also the power ratio of low frequency to high frequency (> 0.1 Hz) of the signal is very low.

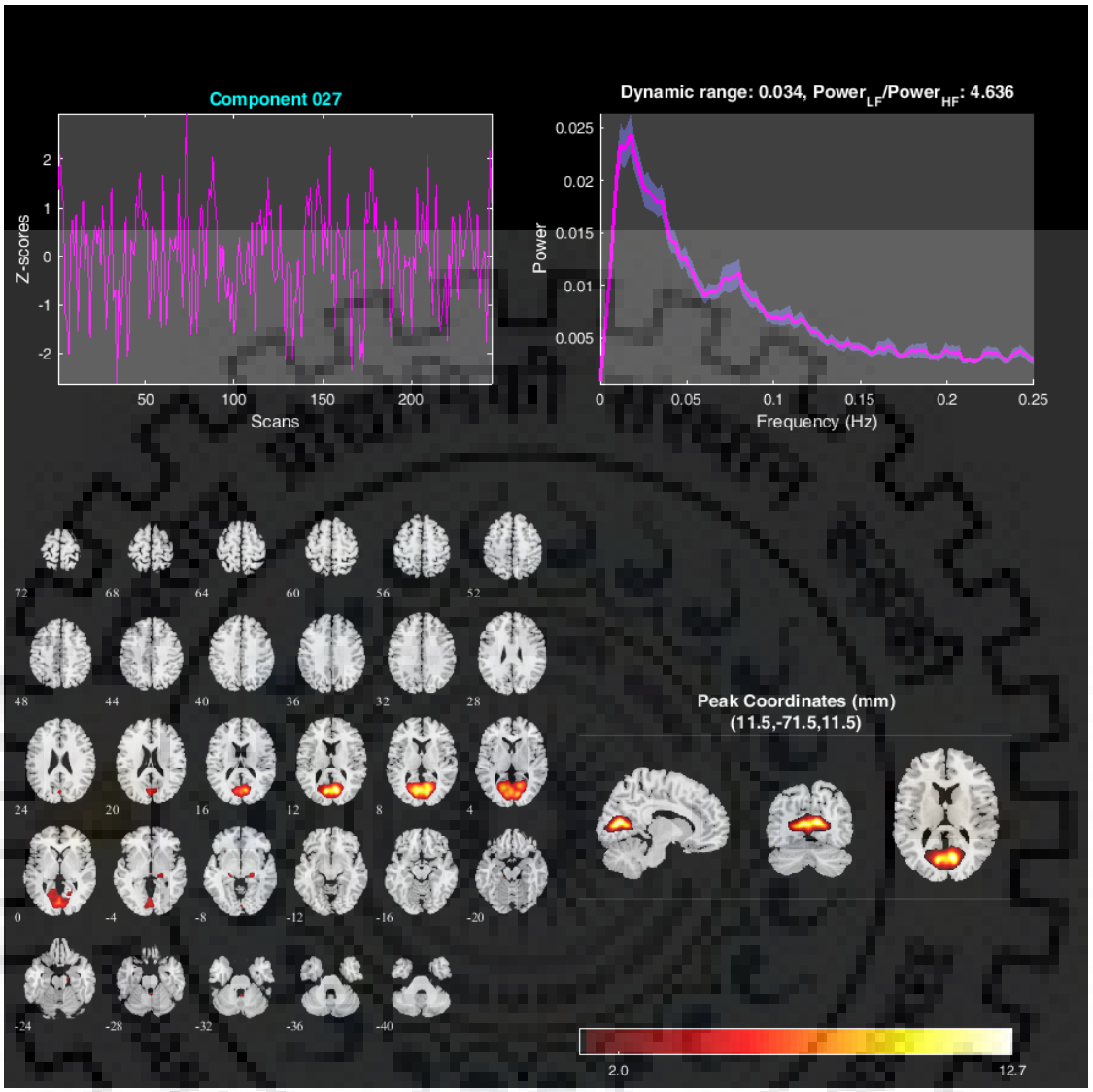

FIGURE 3.3: The label identified for this IC through template matching is default mode network. The component represents a network as most of the power of the activated region lies below the 0.1 Hz frequency range. This IC is labelled incorrectly as the component is lying in the occipital lobe. Therefore it is a visual network.

FIGURE 3.4: The label identified for this IC through template matching is default mode network. The component represents a network as most of the power of the activated region lies below the 0.1 Hz frequency range. This IC is Correctly Labelled.

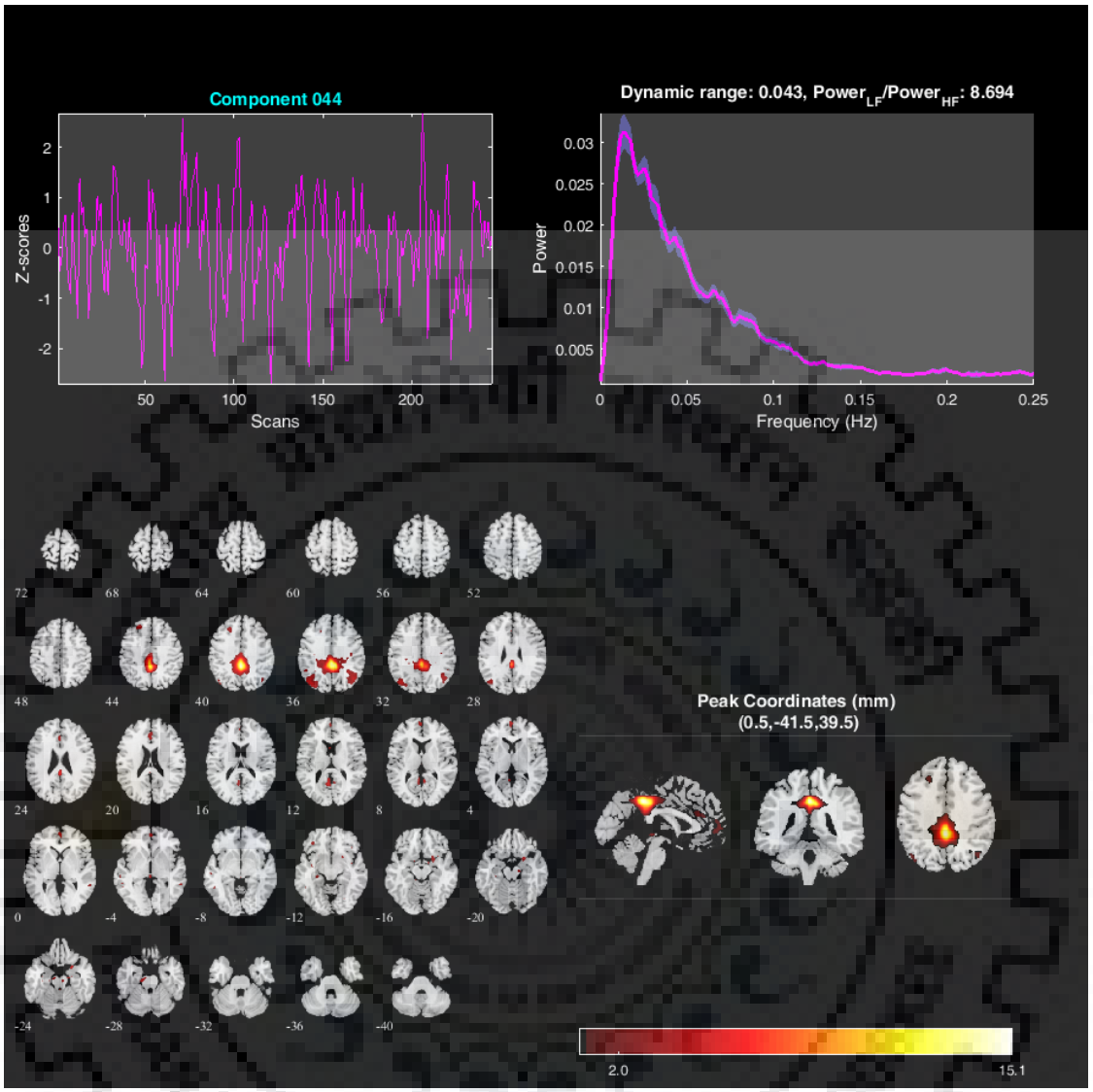

FIGURE 3.5: The label identified for this IC through template matching is executive control network. The component represents a network as most of the power of the activated region lies below the 0.1 Hz frequency range. This component is incorrectly labelled. It is DMN as most of the component is situated in the posterior cingulate cortex.

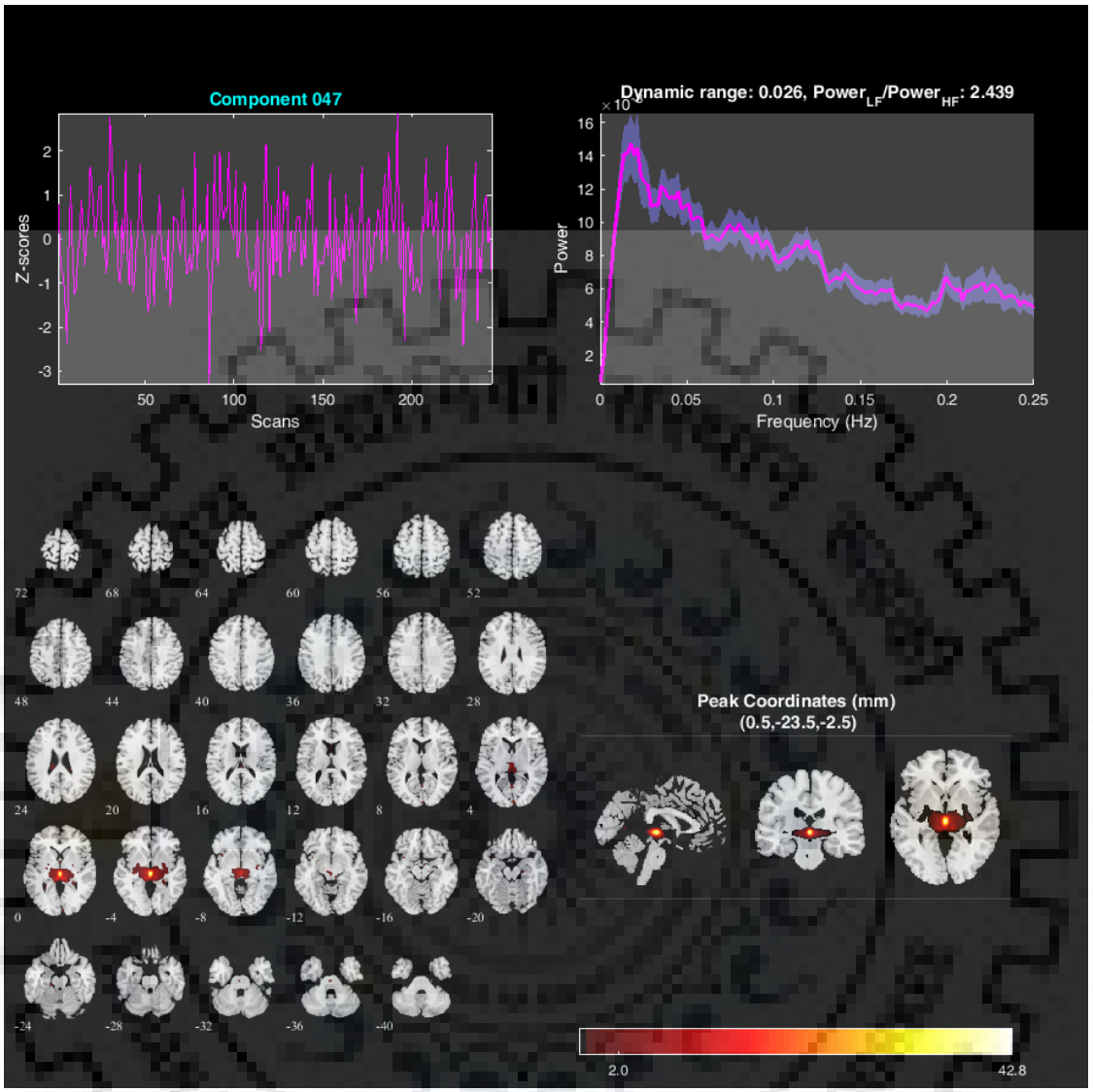

FIGURE 3.6: The label identified for this IC through template matching is sensorimotor network. But this IC is noise as the component is scattered to CSF and white matter and also the power ratio of low frequency to high frequency (> 0.1 Hz) of the signal is very low.

Chapter 4

Proposition of the 3-D CNN Framework

4.1 Development of Dataset

The dataset for the training of the deep learning model is developed from the fMRI data downloaded from the PCP (Preprocessed Connectomes Project) via NITRC website (mentioned in chapter 2). The independent components were extracted from the dataset using ICA and the functional networks and artifacts were separated using the rules mentioned in chapter 3.

The template figures used for the reference during the manual labelling includes Figure 4.1 alongwith Figure 3.1. The following figure shows the network assignment of parcels using an independent dataset, the Human Connectome Project (HCP: 100 unrelated) (Essen et al., 2013). 14 functional networks were identified through network assignment of each parcel using Generalized Louvain method for community detection. The identified functional network topology replicated the spatial mappings of several previously published network partitions (Gordon et al., 2014; Power et al., 2011; Thomas Yeo et al., 2011) (Schultz et al., 2017).

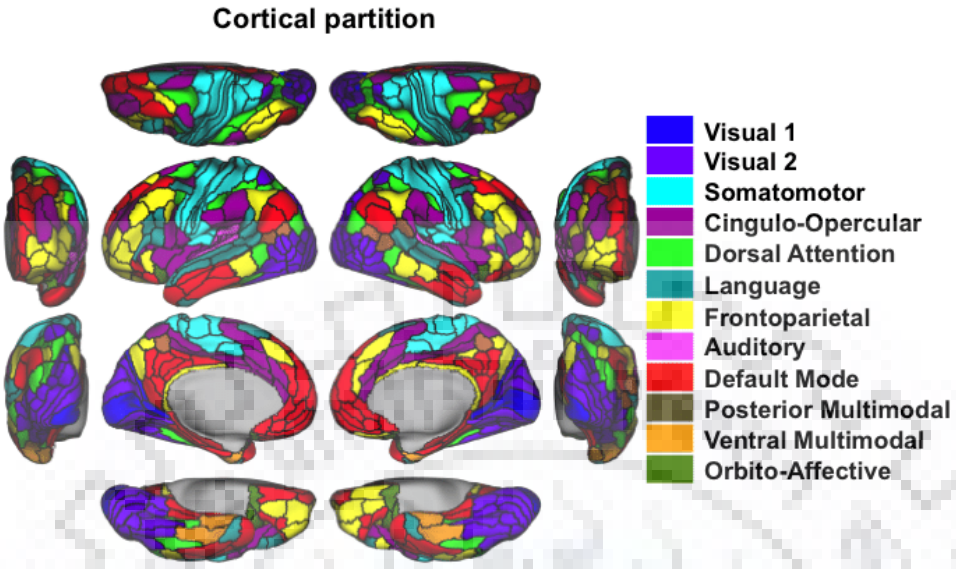

FIGURE 4.1: Resting-state fMRI data was used to create networks for visual interpretation purpose using a community detection algorithm. This resulted in a total of 14 networks. Color indicates the network assignment for each parcel (Schultz et al., 2017).

These networks then were separated into individual 3D images from the 4D form using MATLAB(2019). All the individual functional networks were then grouped together according to the functional networks they represent in separate folders. The folder names represent the labels for the images contained in them. The input data to feed into the 3D-CNN framework is then created using the imageDatastore function of the MATLAB(2019) and accordingly 60% of the data is selected for network 'training' purpose and 40% of the data is left for 'validation' purpose.

4.2 3-D CNN Structure

The studies on automation using machine learning (ML) have shown that a diverse number of complex features can be learnt using deep learning CNNs (Zhao et al., 2018) which can be trained in either supervised or unsupervised fashion according to the problem. However, most of the previous researches related to CNN are 2D-centric,

which most of the time is not optimal for 3D image representation as it may miss the 3D structural information present in the volumetric data. In this work, an improved fully 3D CNN framework of MATLAB(2019a) is used to train the CNN that aims to classify and recognize RSNs reconstructed by Independent Component Analysis method. This 3D convolutional architecture can well extract 3D structural information as intrinsic features. The proposed 3D CNN structure is summarized in Fig. 3. The details of the layers are as follows:

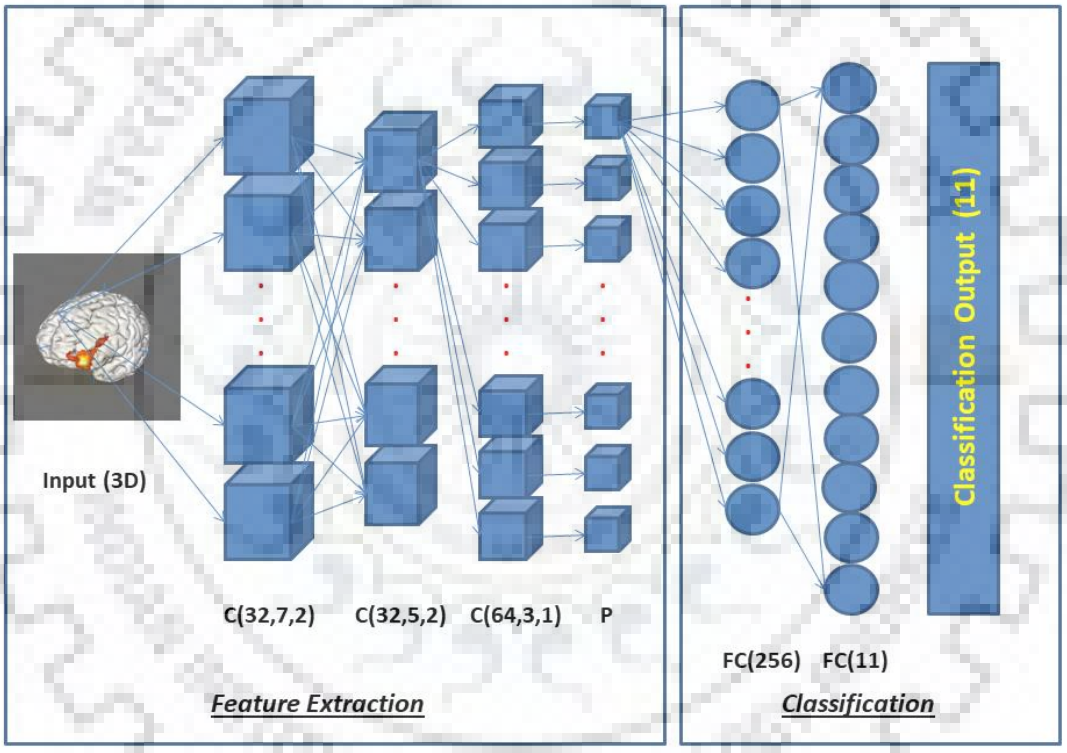

FIGURE 4.2: Structure of 3D CNN used in the work.

4.2.1 Convolutional Layers

The convolutional layers of the proposed CNN is represented as C(f,d,s), where f is the number of filters, also the number of 3D feature maps after convolution; d is the size of the cubic filter and s is the stride. After each convolutional layer a leaky rectified

linear unit (ReLU) as activation unit is used with scaling 0.01. After the training of the CNN, RSNs-specific filters were obtained for each convolutional layers. All the filters were initialized at the beginning such that when each filter slides over the image they extracts certain features from it using convolution. Thus they form feature maps from each extracted feature. The consecutive layers extracts features in the same way from previous layer's feature maps. After the back propagation in each cycle the weights gets updated to extract the most useful features.

4.2.2 Pooling Layers

A pooling layer is used to reduce or down sample the convoluted filters feature maps. By having less spatial information there is a gain computation performance; it also means less parameters, so less chance to over-fit and gets to utilize the translation invariance property of pooling layers (Scherer et al., 2010). Due to this the global shifts in preprocessing steps (such as image registration) and individual shape and size variability of RSNs can be accounted for. This is one of the major advantages of 3D CNN for automatic and robust recognition of RSNs. In this work, a max pooling layer with pooling size of 2 was taken.

4.2.3 Fully Connected Layer and Output Layer

The two layers are functioning as the classification/recognition element in the 3D CNN framework. With well-extracted features from the feature maps as input, 256 nodes were selected for fully connected layer. The output layer contains 11 nodes, each of which uses SoftMax action function to predict and classify the resting state network.

Chapter 5

Results and Discussion

The performance of the 3D CNN model is discussed in this chapter. After the training of the CNN structure the values of weights and biases were updated so that 3d filters can be arranged to identify the independent components with great accuracy. The performance of this work is then evaluated and compared with other techniques such as template matching (correlation scores) and past works.

5.1 Training of 3D CNN

The proposed model was compiled and trained using MATLAB(2019a) software. The dataset consists a total of **3261** NIFTI format 3D images of independent components extracted from individual fMRI scans. Each image was around of 1.03 MB in size and the total size of the dataset was **3.29 GB**. The weights and biases for the convolutional filters were randomly initialized as per the protocol of default options for training the CNN in MATLAB. The 3D CNN structure was trained using the Stochastic Gradient Descent optimizer with momentum (default is **0.9**). A batch size of 100 images was selected. The base learning rate was taken to be **0.001** with a learn rate drop factor of

0.95. The model was trained on CPU (Intel(R) Xeon(R) E5-1650 v3 16 GB memory) for **40 epochs**.

The 3261 independent components were categorized in a total of **10** large scale functional brain networks and 1 artifacts or noise category. The functional brain networks accounted in this work are as follows: Auditory network, Basal Ganglia region/network, Default mode network, Dorsal attention network, Frontoparietal network, Language network, Precuneus region/network, Sensorimotor network, Ventral attention network and Visual network.

5.2 Results

With the fully 3D trained CNN using the data formed using the dataset from the FCP an accuracy of **97.55%** is achieved. Out of the 3261 3D images 40% were used to validate the CNN model. So, the proposed 3D CNN model successfully recognised 1272 images of 1304 total images. The CNN model showed great performance in the identification and recognition of the functional networks extracted using ICA. For the training purpose the dataset not only contained the functional networks spatial maps but also the artifacts (or noise) components so that it can segregate the S-ICs from the N-ICs well.

The training time-line of the CNN structure using MATLAB(2019a) is displayed in figure 5.1 and table 5.1. The training of the CNN network almost took 43 minutes in 17 epochs to train itself for the best performance needed as can be seen in table 5.1.

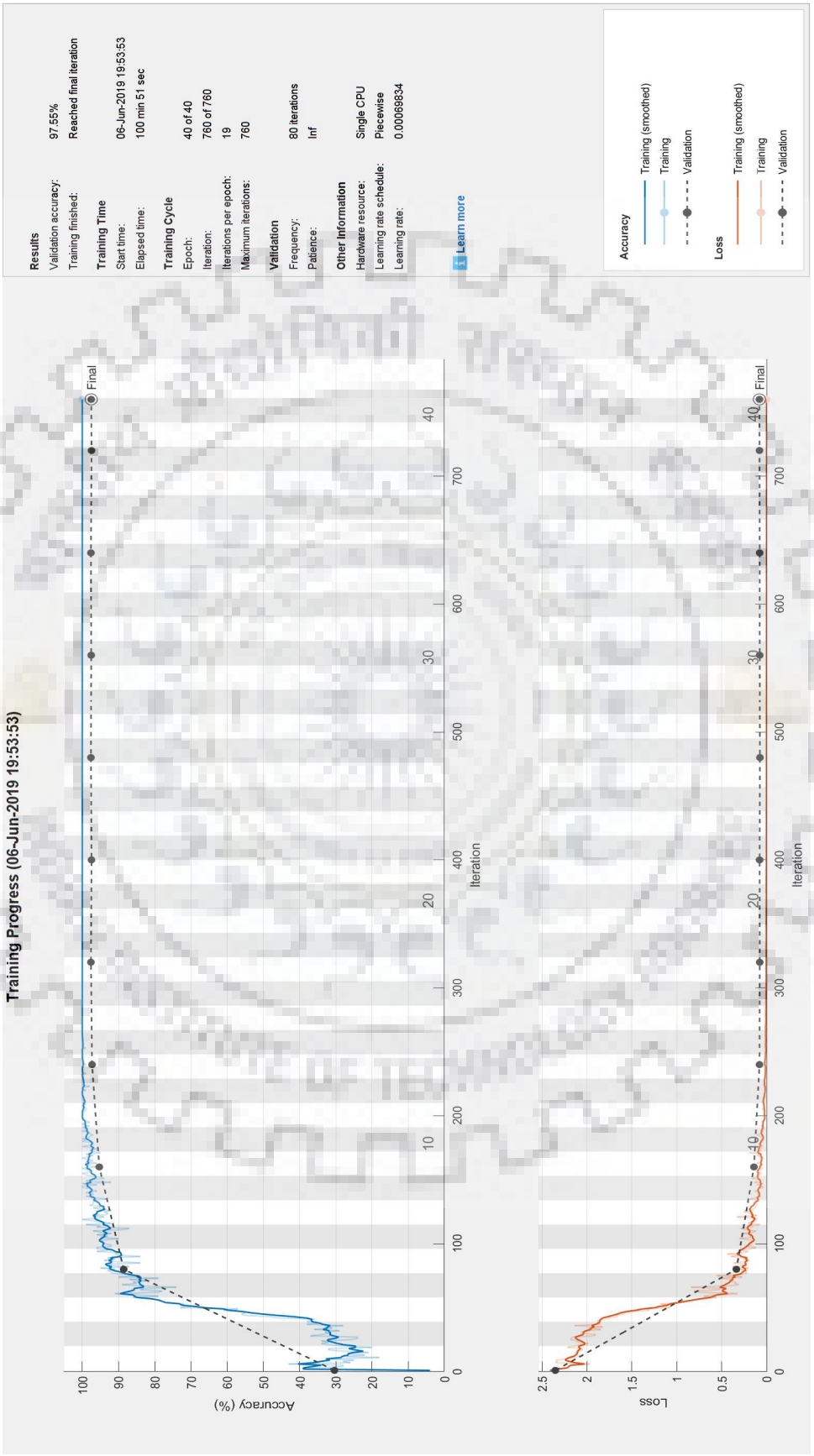

FIGURE 5.1: Training Progress of the CNN model

TABLE 5.1: Learning Progress

Epoch	Time Elapsed (hh:mm:ss)	Mini-batch Accuracy	Validation Accuracy	Mini-batch Loss	Validation Loss	Base Learning Rate
1	00:00:44	4.00%	30.37%	2.4128	2.3525	0.0010
3	00:06:54	73.00%		1.0714		0.0010
5	00:11:14	91.00%	88.57%	0.3049	0.3371	0.0010
6	00:13:44	94.00%		0.1658		0.0010
8	00:19:58	98.00%		0.0745		0.0010
9	00:21:48	96.00%	95.32%	0.0909	0.1415	0.0010
11	00:26:48	100.00%		0.0184		0.0009
13	00:32:23	99.00%	97.32%	0.0319	0.0794	0.0009
14	00:33:38	100.00%		0.0083		0.0009
16	00:39:51	100.00%		0.0061		0.0009
17	00:42:55	100.00%	97.62%	0.0054	0.0770	0.0009
19	00:46:38	100.00%		0.0064		0.0009
22	00:53:25	100.00%	97.47%	0.0062	0.0785	0.0008
24	00:59:36	100.00%		0.0027		0.0008
26	01:03:53	100.00%	97.62%	0.0021	0.0748	0.0008
27	01:06:21	100.00%		0.0017		0.0008
29	01:12:33	100.00%		0.0017		0.0008
30	01:14:21	100.00%	97.55%	0.0012	0.0774	0.0008
32	01:19:18	100.00%		0.0018		0.0007
34	01:24:50	100.00%	97.62%	0.0017	0.0775	0.0007
35	01:26:04	100.00%		0.0013		0.0007
37	01:32:15	100.00%		0.0009		0.0007
38	01:35:19	100.00%	97.47%	0.0015	0.0795	0.0007
40	01:39:02	100.00%		0.0013		0.0007
40	01:40:51	100.00%	97.55%	0.0017	0.0804	0.0007

The convolutional filters after the completion of the training of CNN structure got capable of successfully identifying and recognizing the independent components given as input to the neural network. These filters extracted the specific 3D structural information from the input ICs of fMRI images. The value of the weights of filters stores the information about the edges, surfaces and volumes. The weights of the filters were updated using the leaky ReLU activation function to get smooth output. The CNN structure not only featured out the surface and volumetric information but also the spatial information as the presence of different functional components is based of specific brain regions.

A visual approach of the trained RSNs-specific convolutional filters was taken for the better understanding of the CNN framework. Layer 1 (Figure 5.2) contains 32 different types of filters having a size of 7 x 7 x 7. Each filter convolves with the input image to extract feature maps from it. Layer 2 (Figure 5.3) contains 32 different types of filters having a size of 5 x 5 x 5. Each filter from this layer convolves simultaneously with previous layer's all feature maps to extract new feature maps for the current layer. Layer 3 (Figure 5.4 and 5.5) contains 64 different types of filters having a size of 3 x 3 x 3. Each filter from this layer also extract feature maps using all feature maps from previous layer.

FIGURE 5.2: 3D filters of Convolutional Layer 1

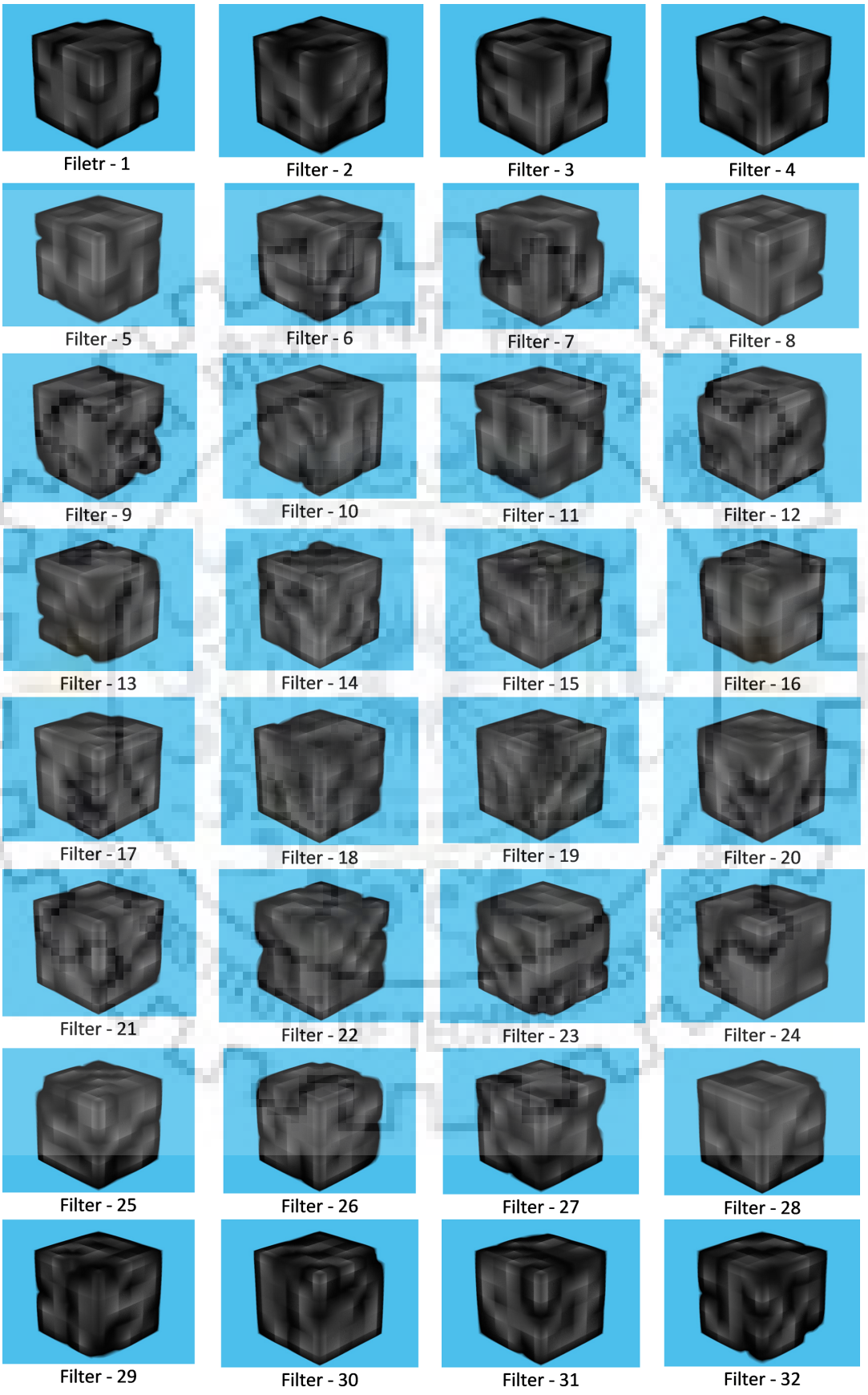

FIGURE 5.3: 3D filters of Convolutional Layer 2

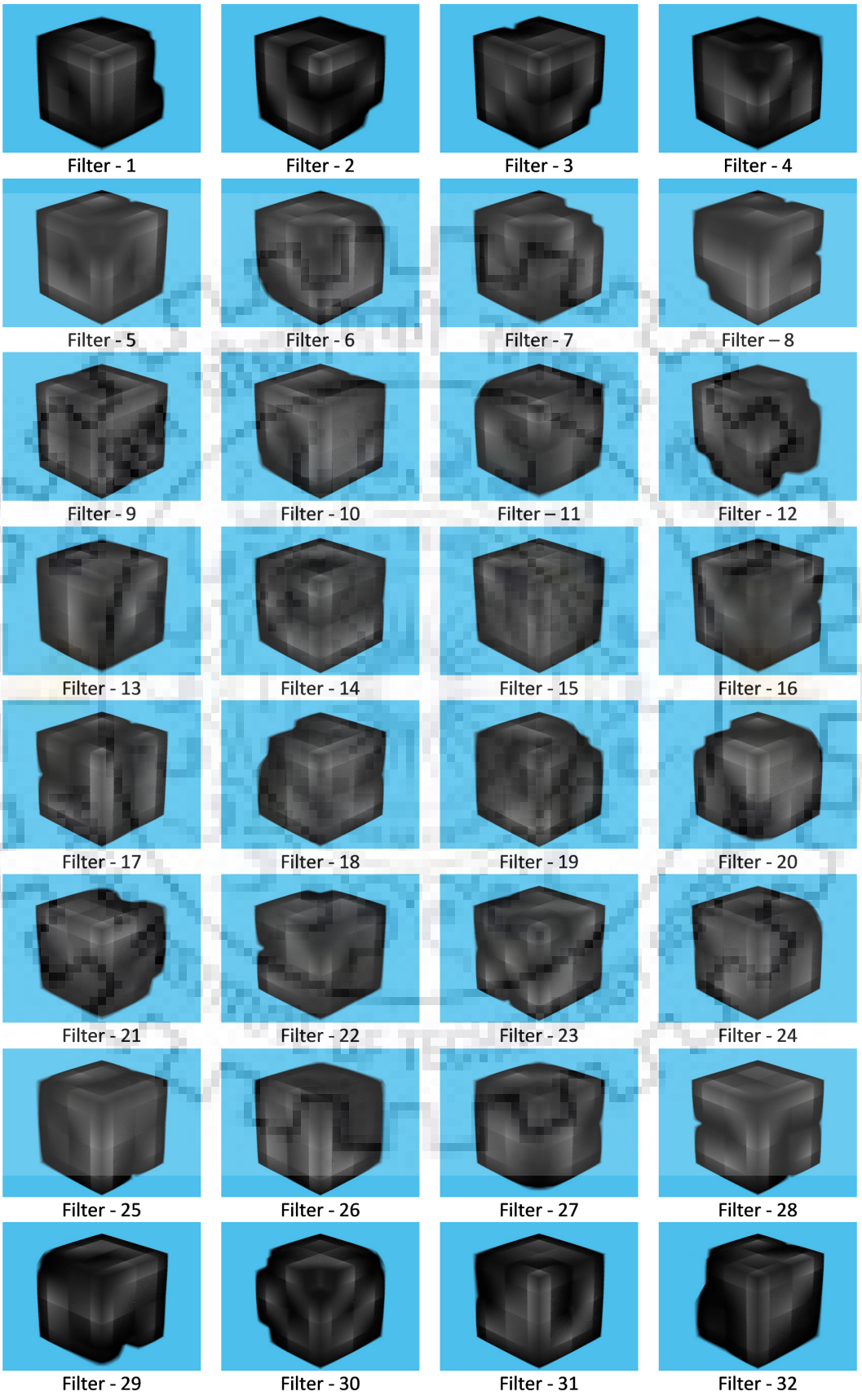

FIGURE 5.4: 3D filters of Convolutional Layer 3

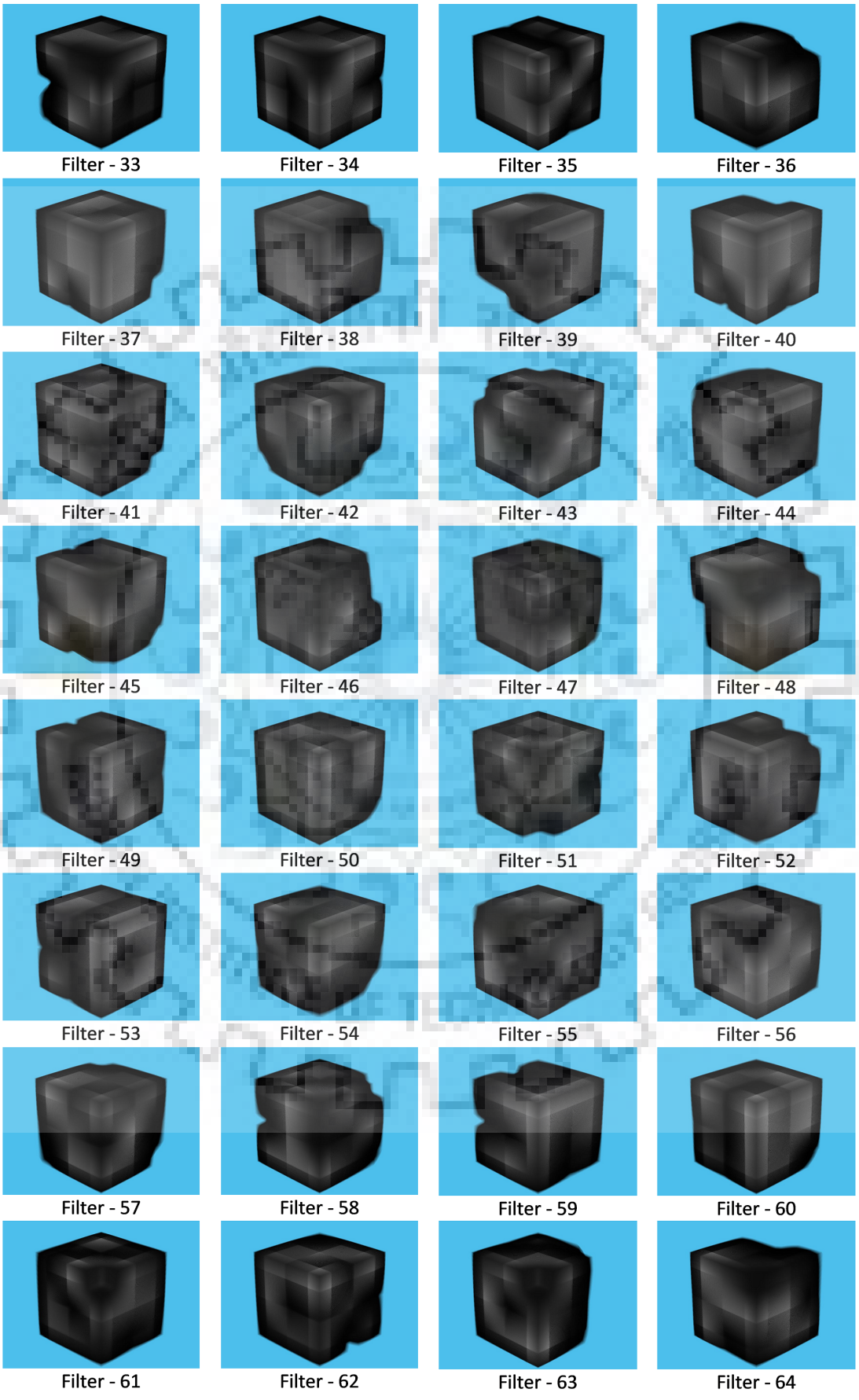

FIGURE 5.5: 3D filters of Convolutional Layer 3

The 3D CNN structure while successfully recognizing the various independent components, correctly labelled the previously incorrectly labelled components using the correlation scores. The CNN structure was able to successfully recognize the minute spatial differences between the functional networks which criteria is majorly lost in correlation and statistical techniques. In statistical methods the recognition of the noise components presents itself to be difficult as the artifacts are not region specific and or shape and sizes. This problem is majorly taken care of with the use of CNN architecture. Some of the ICs correctly recognized by CNN model are listed below.

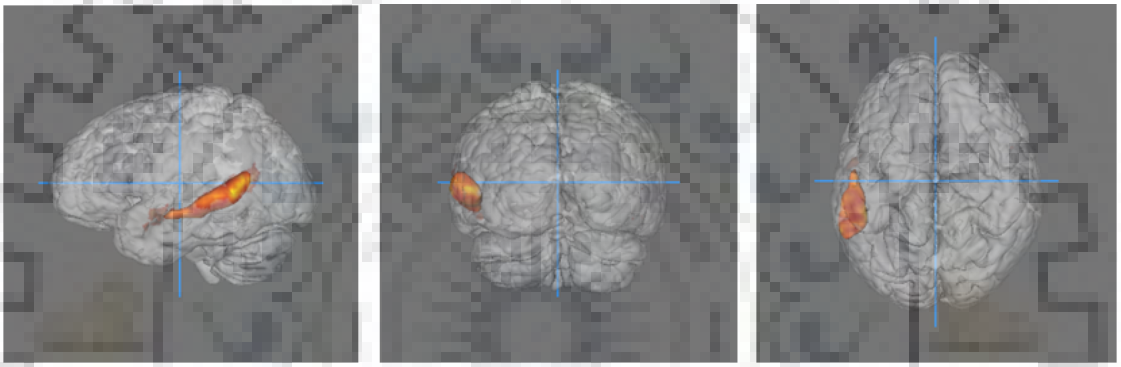

FIGURE 5.6: A component which was labelled as an auditory network using template matching is correctly labelled as a language network using the CNN model

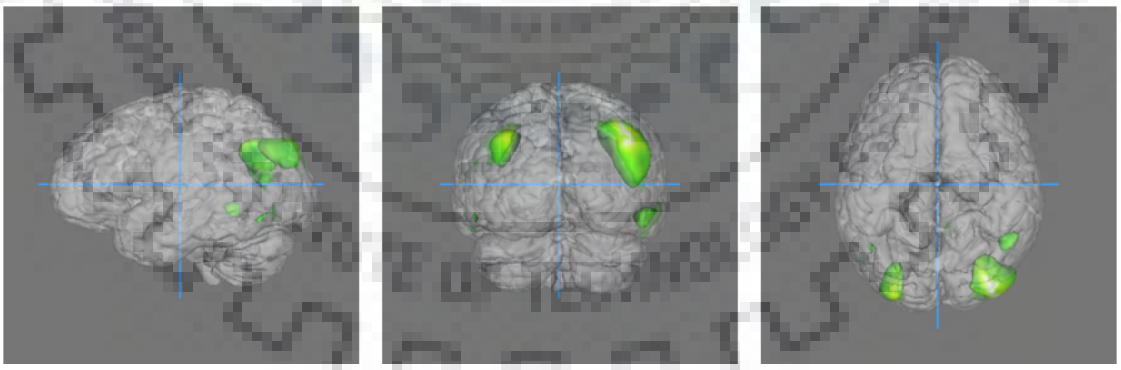

FIGURE 5.7: A component which was labelled as a frontoparietal network using template matching is correctly labelled as a DMN using the CNN model

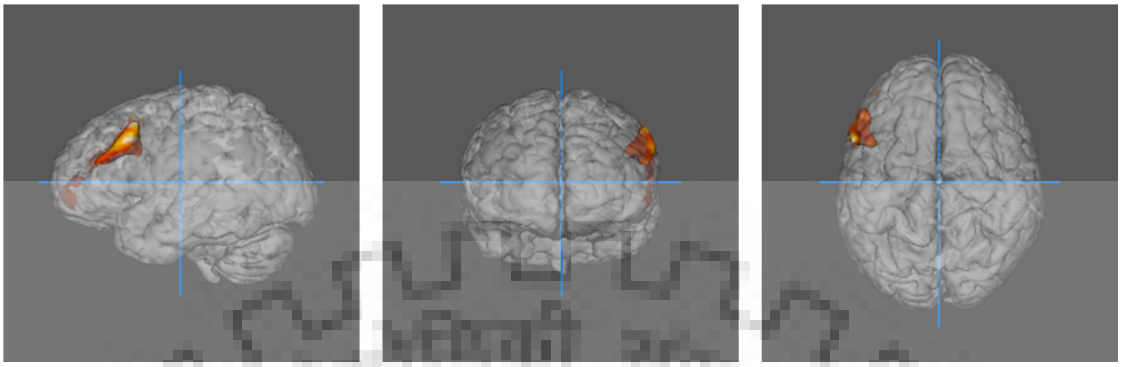

FIGURE 5.8: A component which was labelled as a language network using template matching is correctly labelled as a frontoparietal network using the CNN model

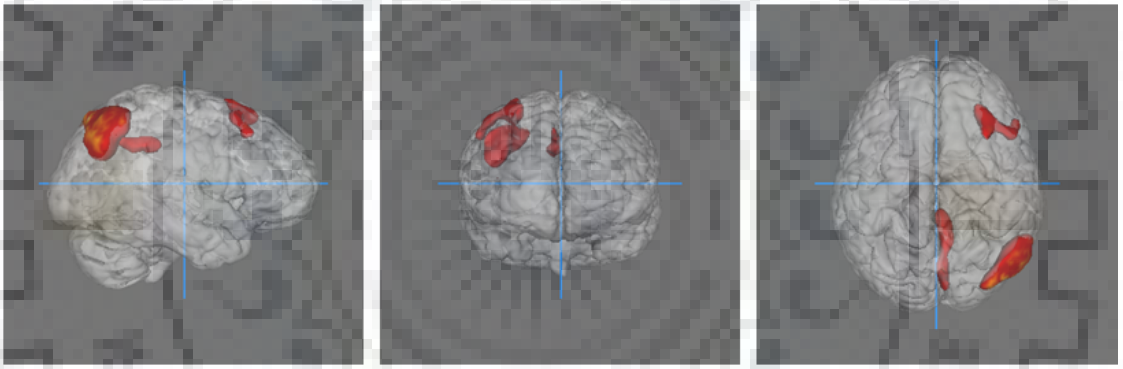

FIGURE 5.9: A component which was labelled as a visual network using template matching is correctly labelled as a frontoparietal network using the CNN model

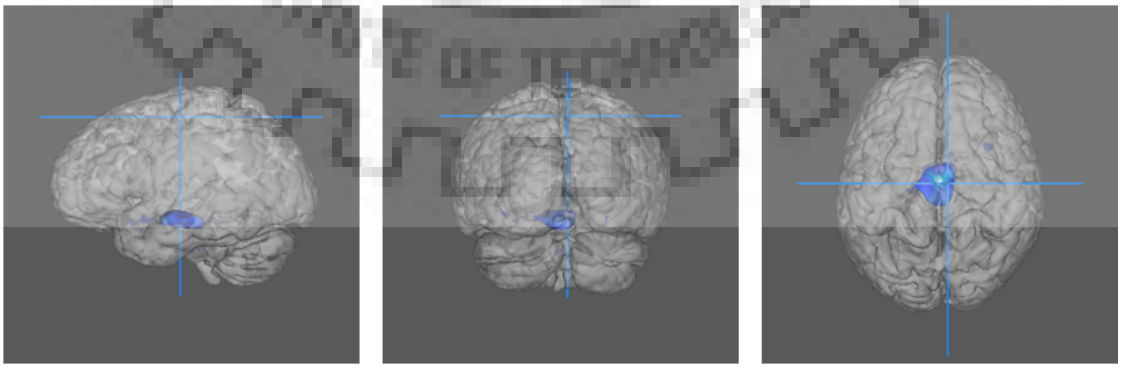

FIGURE 5.10: A component which was labelled as a functional component using template matching is correctly recognized as noise using the CNN model

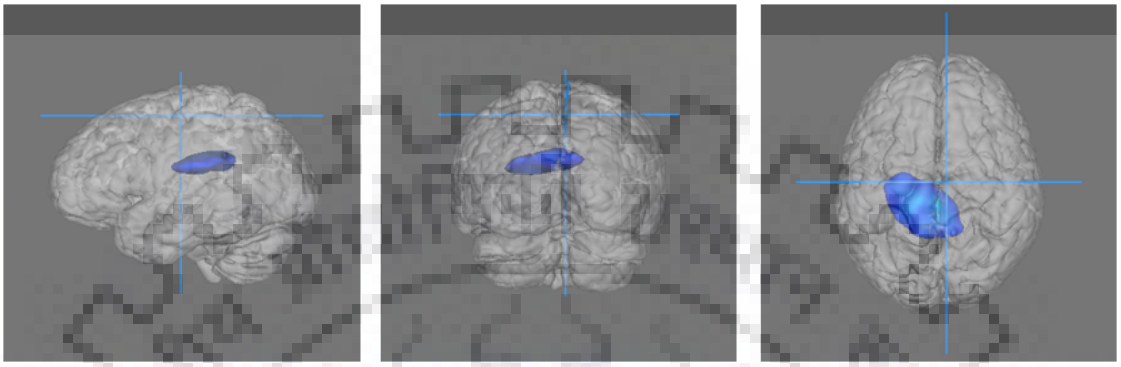

FIGURE 5.11: A component which was labelled as a functional component using template matching is correctly recognized as noise using the CNN model

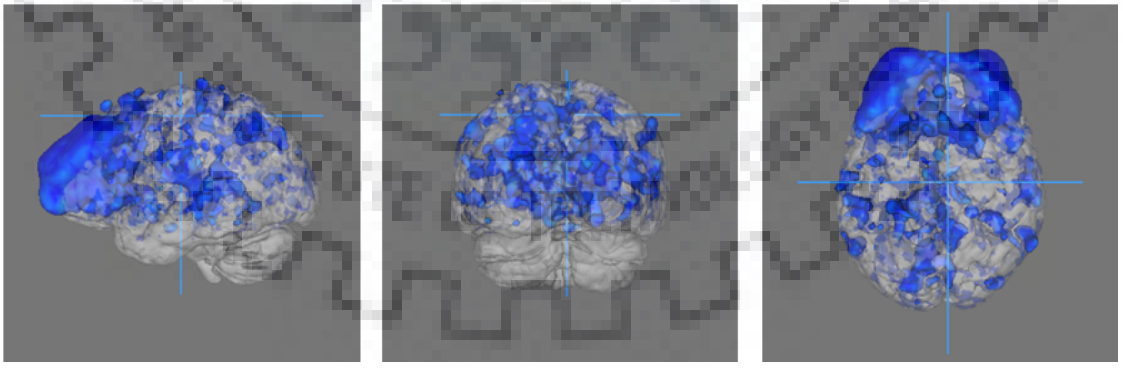

FIGURE 5.12: A component which was labelled as a functional component using template matching is correctly recognized as noise using the CNN model

To make the CNN model more robust and precise it is also trained with artifact components (N-ICs) so that it does not only identify the functional components correctly but also successfully segregate the noise and signal components. This approach turned out to be very successful as it makes the process of identification of components more automatic and human error-free. This is one of the drawbacks of the statistical approaches of automatic labelling as these approaches also recognize and label the noise components based on their output scores (ex. z - scores). Although CNN approach is very promising in the identification of the noise components it is still a challenging issue to segregate the RSNs and artifactual components as these do not have a defined pattern or structure.

To test the universality of the trained fully 3D CNN model it is tested on a different datatset from the ones used to train the model. The data was also taken from the preprocessed connectomes project (PCP). The scans gathered at Carnegie Mellon University, preprocessed using CCS protocol at 1000 functional connectomes project (FCP) website were used to test the robustness of the proposed CNN model. The scans consists of a total of 27 people (14 ASDs and 13 TCs) in the age group of 19 - 40. The independent components of order 100 were extracted using the GICA functionality of GIFT toolbox. The mean of the ICs of the group is taken for the testing of the neural network in identification and recognition of the functional networks. The network showed a remarkable performance in correctly recognizing the networks as noise or functional networks and identifying the correct functional networks with an accuracy of **95.83%**.

Some of the networks were deliberately labelled wrong and some of the networks were identified false during the manual labelling process. The neural network not only identified purportedly wrongly labelled components successfully but also corrected the misidentified components.

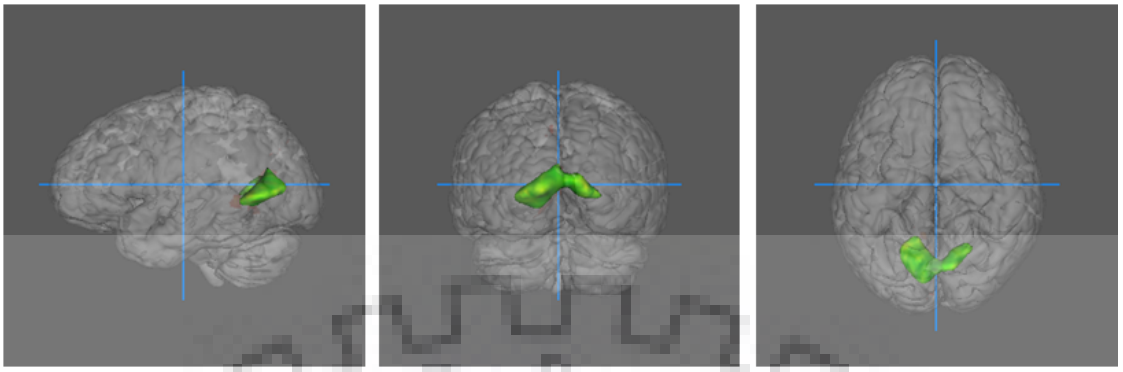

FIGURE 5.13: Resting State Network manually misdentified as DMN correctly recognized as Visual Network by 3D CNN model.

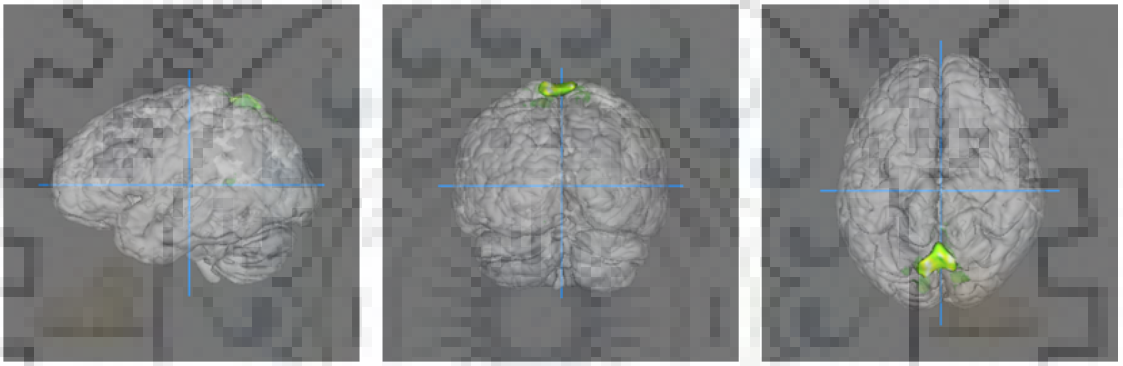

FIGURE 5.14: Resting State Network manually misidentified as sensorimotor network is correctly identified as dorsal attention network by 3D CNN model.

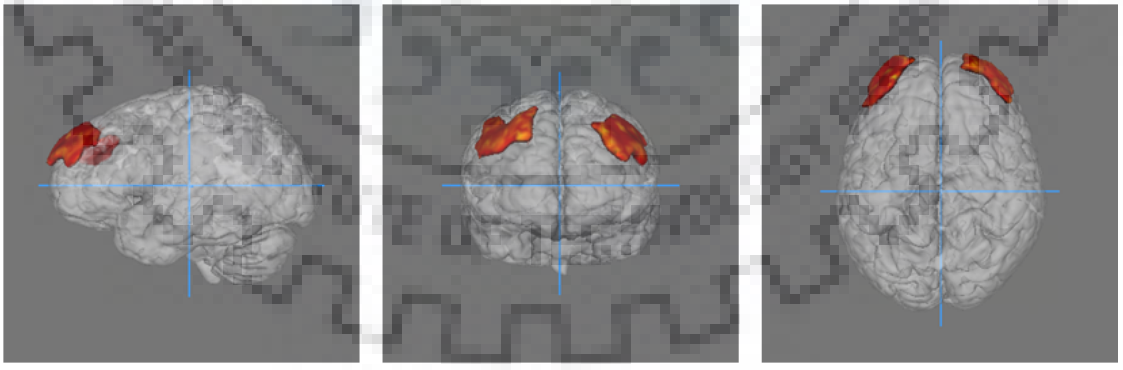

FIGURE 5.15: Resting State Network deliberately labelled as frontoparietal but is correctly identified as ventral attention network by 3D CNN model.

Chapter 6

Conclusion and Future Work

The traditional technique used to identify the resting state networks (RSNs) was overlap based method also known as template matching. In recent years various machine learning techniques were also reported to recognize the RSNs. Earlier 2D CNN learning was approached and then recently 3D CNN learning was approached (Zhao et al., 2018). The reported accuracy with overlap based method was found out around 85% (Zhao et al., 2018) and the voxnet based 3D CNN model achieved an accuracy of 94.61% (Zhao et al., 2018). In this work the proposed 3D CNN model achieved an accuracy of 97.55% and also was able to recognize the noise components effectively. In addition to this the model's robustness is tested with different dataset and found out to performed very well. It is concluded that the CNN based machine learning techniques outperform the traditional methods of identification and segregation of RSNs. Despite a great performance of the proposed CNN framework, however, there also exist challenges and limitations to it. First, the training datset preparation is a difficult issue for training the CNN networks. As can be seen, the RSNs would have to be manually labelled before it can be used for the training purposes which is a very time consuming process to manually label thousands of functional network maps, among which 40 - 70 % of them are RSNs. Also, there always lies unavoidable manual labelling mistakes and inter-rater variability of labels. For these problems a reliable and fully or semi-automated CNN

networks should be explored in the near future to accommodate larger datesets and improved training accuracy.

Secondly, only large scale brain networks were considered in this work which is a testing platform for the proposed 3D CNN framework. As the understanding of cortical associations and the activation of brain region increases the accuracy of resting state networks labelling increases. In the future, more number of functional networks must be incorporated in the building of a more efficient and insightful CNN network as hundreds of networks are already found out in the researches and large scale neuroimaging projects (Zhao et al., 2018).

Finally, this deep learning approach gives a way towards the speed and automation (free from human error) of recognition of resting state networks which would lead to a better understanding of altered brain networks in degenerative brain diseases and disorders.

Bibliography

Bharat Biswal, F. Zerrin Yetkin, Victor M. Haughton, and James S. Hyde. Functional connectivity in the motor cortex of resting human brain using echo-planar mri. *Magnetic Resonance in Medicine*, 34:537–541, 1995.

Bharat Biswal, F Zerrin Yetkin, Victor Haughton, and James Hyde. Functional connectivity in the motor cortex of resting human brain using echo-planar mri. *Magnetic Resonance in Medicine*, 34:537–541, 1998.

Cécile Bordier, Michel Dojat, and Pierre Lafaye de Micheaux. Temporal and spatial independent component analysis for fmri data sets embedded in a r package. *journal of Statistical Software*, 44, 2010.

R. Cameron Craddock and Pierre Bellec. Preprocessed connectomes project. `http://preprocessed-connectomes-project.org/`, 2019.

Michael D Greicius, Benjamin H Flores, Vinod Menon, Gary H Glover, Hugh Solvason, Heather Kenna, Allan L Reiss, and Alan Schatzberg. Resting-state functional connectivity in major depression: Abnormally increased contributions from subgenual cingulate cortex and thalamus. *Biological psychiatry*, 62:429–37, 10 2007. doi: 10.1016/j.biopsych.2006.09.020.

Eric Egolf, KA Kiehl, and VD Calhoun. Group ica of fmri toolbox (gift). *Proc. HBM Budapest, Hungary*, 2004.

David C. Van Essen, Stephen M. Smith, Deanna M. Barch, Timothy E.J. Behrens, Essa Yacoub, and Kamil Ugurbil. The wu-minn human connectome project: An

overview. *NeuroImage*, 80:62 – 79, 2013. ISSN 1053-8119. doi: https://doi.org/10.1016/j.neuroimage.2013.05.041. URL `http://www.sciencedirect.com/science/article/pii/S1053811913005351`. Mapping the Connectome.

Anja Fengler. *How the brain attunes to sentence processing*. PhD thesis, University of Leipzig, Jahnallee 59, 04109 Leipzig, Germany, 01 2016.

Karl J. Friston. Functional and effective connectivity in neuroimaging: A synthesis. *Human Brain Mapping*, 2:56–78, 1994.

Karl J. Friston, Steven Williams, Robert Howard, Richard S. J. Frackowiak, and Robert Turner. Movement-related effects in fmri time-series. *Magnetic Resonance in Medicine*, 35(3):346–355, 1996. doi: 10.1002/mrm.1910350312. URL `https://onlinelibrary.wiley.com/doi/abs/10.1002/mrm.1910350312`.

Evan M. Gordon, Timothy O. Laumann, Babatunde Adeyemo, Jeremy F. Huckins, William M. Kelley, and Steven E. Petersen. Generation and Evaluation of a Cortical Area Parcellation from Resting-State Correlations. *Cerebral Cortex*, 26(1):288–303, 2014. doi: 10.1093/cercor/bhu239. URL `https://doi.org/10.1093/cercor/bhu239`.

Michael D. Greicius, Gaurav Srivastava, Allan L. Reiss, and Vinod Menon. Default-mode network activity distinguishes alzheimer's disease from healthy aging: evidence from functional mri. *Proceedings of the National Academy of Sciences of the United States of America*, 101:4637–4642, 2004.

Robert Kelly, George Alexopoulos, Zhishun Wang, Faith Gunning-Dixon, Christopher Murphy, Sarah Morimoto, Theodora Kanellopoulos, Zhiru Jia, Kelvin O Lim, and Matthew Hoptman. Visual inspection of independent components: Defining a procedure for artifact removal from fmri data. *Journal of neuroscience methods*, 189: 233–45, 04 2010. doi: 10.1016/j.jneumeth.2010.03.028.

Van Dijk KR, Hedden T, Venkataraman A, Evans KC, Lazar SW, and Buckner RL. Intrinsic functional connectivity as a tool for human connectomics: theory, properties and optimization. *journal of Neurophysiology*, 34:297–321, 2010.

Fox MD, Snyder AZ, Vincent JL, and Raichle ME. Intrinsic fluctuations within cortical systems account for intertrial variability in human behavior. *Neuron*, 56:171–184, 2007.

Logothetis NK and Pfeuffer J. On the nature of the bold fmri contrast mechanism. *Magnetic Resonance Imaging*, 22:586–595, 2004.

Russell A. Poldrack, Jeanette A. Mumford, and Thomas E. Nichols. *Handbook of Functional MRI Data Analysis*. Cambridge University Press, 2011.

Jonathan D. Power, Alexander L. Cohen, Steven M. Nelson, Gagan S. Wig, Kelly Anne Barnes, Jessica A. Church, Alecia C. Vogel, Timothy O. Laumann, Fran M. Miezin, Bradley L. Schlaggar, and Steven E. Petersen. Functional network organization of the human brain. *Neuron*, 72(4):665 – 678, 2011. ISSN 0896-6273. doi: https://doi.org/10.1016/j.neuron.2011.09.006. URL `http://www.sciencedirect.com/science/article/pii/S0896627311007926`.

Mueller S, Wang D, Fox MD, Yeo BT, Sepulcre J, Sabuncu MR, Shafee R, Lu J, and Liu H. Individual variability in functional connectivity architecture of the human brain. *Neuron*, 77:586–595, 2013.

Dominik Scherer, Andreas Müller, and Sven Behnke. Evaluation of pooling operations in convolutional architectures for object recognition. In *Artificial Neural Networks - ICANN 2010*, pages 92–101, Berlin, Heidelberg, 2010. Springer Berlin Heidelberg. ISBN 978-3-642-15825-4.

Douglas H. Schultz, Takuya Ito, Levi I. Solomyak, Richard H. Chen, Ravi D. Mill, Kaustubh R. Kulkarni, and Michael W. Cole. Global connectivity of the frontoparietal cognitive control network is related to depression symptoms in undiagnosed

individuals. *bioRxiv*, 2017. doi: 10.1101/185306. URL https://www.biorxiv.org/content/early/2017/09/06/185306.

Stephen M. Smith, Peter T. Fox, Karla L. Miller, David C. Glahn, P. Mickle Fox, Clare E. Mackay, Nicola Filippini, Kate E. Watkins, Roberto Toro, Angela R. Laird, and Christian F. Beckmann. Correspondence of the brain's functional architecture during activation and rest. *Proceedings of the National Academy of Sciences*, 106 (31):13040–13045, 2009. ISSN 0027-8424. doi: 10.1073/pnas.0905267106. URL https://www.pnas.org/content/106/31/13040.

B. T. Thomas Yeo, Fenna M. Krienen, Jorge Sepulcre, Mert R. Sabuncu, Danial Lashkari, Marisa Hollinshead, Joshua L. Roffman, Jordan W. Smoller, Lilla Zöllei, Jonathan R. Polimeni, Bruce Fischl, Hesheng Liu, and Randy L. Buckner. The organization of the human cerebral cortex estimated by intrinsic functional connectivity. *journal of Neurophysiology*, 106(3):1125–1165, 2011. doi: 10.1152/jn.00338.2011. URL https://doi.org/10.1152/jn.00338.2011. PMID: 21653723.

Petr Tichavsky, Zbyněk Koldovský, and Erkki Oja. Performance analysis of the fastica algorithm and cramér-rao bounds for linear independent component analysis. *Signal Processing, IEEE Transactions on*, 54:1189 – 1203, 05 2006. doi: 10.1109/TSP.2006.870561.

Svyatoslav Vergun, Wolfgang Gaggl, Veena A. Nair, Joshua I. Suhonen, Rasmus M. Birn, Azam S. Ahmed, M. Elizabeth Meyerand, James Reuss, Edgar A. DeYoe, and Vivek Prabhakaran. Classification and extraction of resting state networks using healthy and epilepsy fmri data. *frontiers in Neuroscience*, 2016. URL https://doi.org/10.3389/fnins.2016.00440.

Yu Zhao, Qinglin Dong, Shu Zhang, Wei Zhang, Hanbo Chen, Xi Jiang, Lei Guo, Xintao Hu, Junwei Han, and Tianming Liu. Automatic recognition of fmri-derived functional networks using 3-d convolutional neural networks. *IEEE TRANSACTIONS ON BIOMEDICAL ENGINEERING*, 69, 2018.